Theoretical modeling of the interface recombination effect on the performance of III–V tandem solar cells

Lin Guijiang(林桂江)[1,2,†], Wu Jyhchiarng(吴志强)[2], and Huang Meichun(黄美纯)[1]

(1 Department of Physics, Xiamen University, Xiamen 361005, China)
(2 Xiamen San'an Optoelectronics Co Ltd, Xiamen 361009, China)

Abstract: A typical GaInP/GaInAs/Ge tandem solar cell structure operating under AM0 illumination is proposed, and the current–voltage curves are calculated for different recombination velocities at both front and back-surfaces of the three subcells by using a theoretical model including optical and electrical modules. It is found that the surface recombination at the top GaInP cell is the main limitation for obtaining high efficiency tandem solar cells.

Key words: interface recombination; GaInP/GaInAs/Ge; tandem solar cell; AM0 illumination
DOI: 10.1088/1674-4926/31/8/082004 **PACC:** 7360F; 7290; 8630J

1. Introduction

Presently, GaInP/GaInAs/Ge triple-junction solar cells grown by metal-organic vapor-phase epitaxy (MOVPE) are the high efficiency solar cells for space applications in mass production[1,2]. The GaInP and GaInAs subcells are grown on germanium substrate, with more than twenty different layers and corresponding interfaces for a whole tandem solar cell structure[3]. Minority carrier recombination at these interfaces is a major factor limiting the efficiency. In practice, it is difficult to achieve low recombination velocities in solar cells because of high doping levels and interface diffusion. A detailed understanding of the impact of the interface recombination effect is necessary to effectively design ideal solar cells.

Ghannam *et al.*[4] have discussed the impact of interface recombination on the open-circuit voltage and efficiency of a tandem cell operating under AM1.5 illumination, and Kurtz *et al.*[5] have experimentally studied the effects of passivation for front and back GaInP solar cells. In this paper, a closer analysis and computation of the interface recombination effect on both the photocurrent and photovoltage of GaInP, GaInAs and Ge subcells operating under AM0 illumination are carried out, by using a rigorous model including optical and electrical modules.

2. Theoretical approach

A schematic of a typical lattice-matched GaInP/GaInAs/Ge solar cell is shown in Fig. 1. It consists of the series connection of an n on p GaInP junction on the top of an n/p GaInAs junction which lies on an n/p Ge junction.

The spectrum of sunlight striking the front of the cell includes ultraviolet, visible, and infrared light. The absorption coefficient for short-wavelength light is quite large, and most of the blue light is absorbed very close to the front of the GaInP cell. Light with energy close to, but above, the GaInP band edge is weakly absorbed throughout the cell and a large part reaches the GaInAs cell. Sub-band-gap light passes through the front cell and is absorbed in the next one, and so on. The photocarriers generated will diffuse inside the cell until they are either collected at the p–n junction or recombined with a majority carrier, either by bulk or interface recombination. The efficiency of a solar cell is increased when all the photocarriers are collected at the junction instead of being recombined elsewhere. Thus, recombination at the front and back of the cell affects the efficiency of the cell.

At the first level, multi-junction cells behave like homojunction cells in series, and their open circuit voltage is the sum of the voltages of the subcells, while their short circuit current is that of the subcells with the smallest current. Hence, the performance of a multi-junction cell can be obtained from the performance of each subcell evaluated independently. For each subcell, the load current density J is represented by the superposition of two diode currents and the photogenerated current,

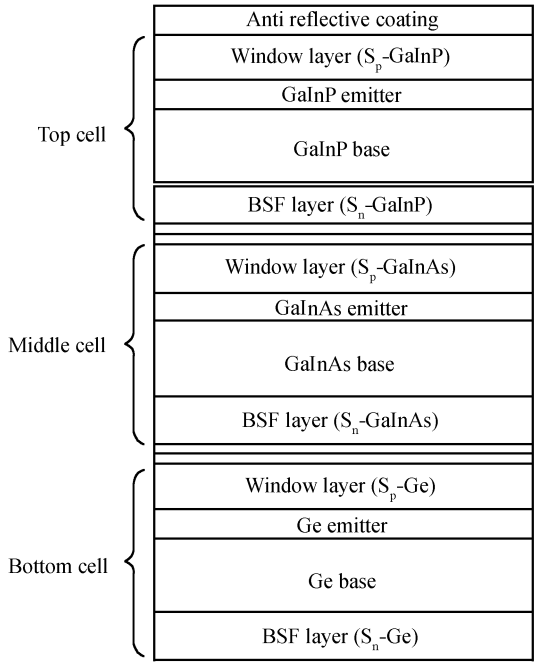

Fig. 1. Solar cell structure used for simulation.

† Corresponding author. Email: linguijiang@sanan-e.com
Received 26 January 2010, revised manuscript received 21 March 2010

$$J = J_{\rm ph} - J_{01}(\mathrm{e}^{qV/kT} - 1) - J_{02}(\mathrm{e}^{qV/2kT} - 1), \tag{1}$$

where $J_{\rm ph}$ is the photocurrent density, J_{01} is the ideal dark saturation current component, and J_{02} is the space charge non-ideal dark saturation current component.

The photocurrent density is given by the sum of the photocurrents generated in the emitter, the base and the depleted region of the cell. Similarly, the dark current density is given by the sum of the dark currents generated in the emitter, the base and the depleted region of the cell[6, 7]. We have

$$J_{\rm ph} = J_{\rm emitter} + J_{\rm base} + J_{\rm depleted}, \tag{2}$$

$$J_{\rm emitter} = \frac{qF(1-R)\alpha L_{\rm p}}{(\alpha L_{\rm p})^2 - 1} \times \left\{ \frac{\dfrac{S_{\rm p}L_{\rm p}}{D_{\rm p}} + \alpha L_{\rm p} - \mathrm{e}^{-\alpha(d_{\rm e}-W_{\rm n})}\left(\dfrac{S_{\rm p}L_{\rm p}}{D_{\rm p}}\cosh\left[(d_{\rm e}-W_{\rm n})/L_{\rm p}\right] + \sinh\left[(d_{\rm e}-W_{\rm n})/L_{\rm p}\right]\right)}{\dfrac{S_{\rm p}L_{\rm p}}{D_{\rm p}}\sinh\left[(d_{\rm e}-W_{\rm n})/L_{\rm p}\right] + \cosh\left[(d_{\rm e}-W_{\rm n})/L_{\rm p}\right]} - \alpha L_{\rm p}\mathrm{e}^{-\alpha(d_{\rm e}-W_{\rm n})} \right\}, \tag{3}$$

$$J_{\rm base} = \frac{qF(1-R)\alpha L_{\rm n}}{(\alpha L_{\rm n})^2 - 1}\mathrm{e}^{-\alpha(d_{\rm b}-W_{\rm n}+W)} \times \left\{ \alpha L_{\rm n} - \frac{\dfrac{S_{\rm n}L_{\rm n}}{D_{\rm n}}\left(\cosh\left[(d_{\rm e}-W_{\rm n})/L_{\rm n}\right] - \mathrm{e}^{-\alpha(d_{\rm b}-W_{\rm p})}\right) + \sinh\left[(d_{\rm b}-W_{\rm p})/L_{\rm n}\right] + \alpha L_{\rm n}\mathrm{e}^{-\alpha(d_{\rm b}-W_{\rm p})}}{\dfrac{S_{\rm n}L_{\rm n}}{D_{\rm n}}\sinh\left[(d_{\rm b}-W_{\rm p})/L_{\rm n}\right] + \cosh\left[(d_{\rm b}-W_{\rm p})/L_{\rm n}\right]} \right\}, \tag{4}$$

$$J_{\rm depleted} = qF(1-R)\mathrm{e}^{-\alpha(d_{\rm e}-W_{\rm n})}\left(1 - \mathrm{e}^{-\alpha W}\right), \tag{5}$$

$$J_{01} = J_{01,\rm emitter} + J_{01,\rm base}, \tag{6}$$

$$J_{01,\rm emitter} = q\frac{n_{\rm i}^2}{N_{\rm D}}\frac{D_{\rm p}}{L_{\rm p}}\left\{\frac{S_{\rm p}L_{\rm p}/D_{\rm p}\cosh\left[(d_{\rm e}-W_{\rm n})/L_{\rm p}\right] + \sinh\left[(d_{\rm e}-W_{\rm n})/L_{\rm p}\right]}{S_{\rm p}L_{\rm p}/D_{\rm p}\sinh\left[(d_{\rm e}-W_{\rm n})/L_{\rm p}\right] + \cosh\left[(d_{\rm e}-W_{\rm n})/L_{\rm p}\right]}\right\}, \tag{7}$$

$$J_{01,\rm base} = q\frac{n_{\rm i}^2}{N_{\rm A}}\frac{D_{\rm n}}{L_{\rm n}}\left\{\frac{S_{\rm n}L_{\rm n}/D_{\rm n}\cosh\left[(d_{\rm b}-W_{\rm p})/L_{\rm n}\right] + \sinh\left[(d_{\rm b}-W_{\rm p})/L_{\rm n}\right]}{S_{\rm n}L_{\rm n}/D_{\rm n}\sinh\left[(d_{\rm b}-W_{\rm p})/L_{\rm n}\right] + \cosh\left[(d_{\rm b}-W_{\rm p})/L_{\rm n}\right]}\right\}, \tag{8}$$

$$J_{02} = \frac{Wn_{\rm i}}{2(V_{\rm d}-V)\tau}, \tag{9}$$

where q is the electron charge, F is the incident photon flux, α is the optical absorption coefficient, and R is the reflectance of the anti-reflective coating. $n_{\rm i}$ is the intrinsic carrier concentration, and $N_{\rm A}$ and $N_{\rm D}$ are the concentrations of acceptors and donors. $d_{\rm e}$ is the emitter thickness, and $d_{\rm b}$ is the base thickness. $L_{\rm p}$ is the hole diffusion length in the emitter, and $L_{\rm n}$ is the electron diffusion length in the base. $S_{\rm p}$ is the hole surface recombination velocity in the emitter, and $S_{\rm n}$ is the electron surface recombination velocity in the base. $D_{\rm p}$ is the hole diffusion coefficient in the emitter, $D_{\rm n}$ is the electron diffusion coefficient in the base, and τ is the nonradiative carrier lifetime. The build-in voltage $V_{\rm d}$ of the junction, the thickness of the depleted layer in the emitter $W_{\rm n}$, the thickness of the depleted layer in the base $W_{\rm p}$, and the total depleted zone thickness W[8] are given by

$$V_{\rm d} = kT\lg\frac{N_{\rm D}N_{\rm A}}{n_{\rm i}^2}, \tag{10}$$

$$W = \sqrt{2\varepsilon\frac{N_{\rm D}+N_{\rm A}}{N_{\rm D}N_{\rm A}}(V_{\rm d}-V-2kT)}, \tag{11}$$

$$W_{\rm n} = W/(1+N_{\rm D}/N_{\rm A}), \tag{12}$$

$$W_{\rm p} = W - W_{\rm n}. \tag{13}$$

where k is the Boltzmann constant, ε the dielectric constant, and T the temperature (T = 25 ℃ was used in this paper). It is important to note that F and α depend on the wavelength, whereas $D_{\rm p}$, $D_{\rm n}$, $L_{\rm p}$, $L_{\rm n}$ and τ depend on the doping concentration[4].

The optical modeling proposed in this paper is based on the transfer matrix formalism. It allows calculation of the incident optical spectrum on each subcell from the solar cell spectrum. Each layer of the multi-junction is described by a transfer matrix M which is defined by

$$M = \begin{pmatrix} M_{0,0} & M_{0,1} \\ M_{1,0} & M_{1,1} \end{pmatrix} = \begin{pmatrix} \cos d\,\dfrac{2\pi\,(n - i\lambda\alpha/4\pi)}{\lambda} & i\,\dfrac{\sin d\,\dfrac{2\pi\,(n - i\lambda\alpha/4\pi)}{\lambda}}{n - i\lambda\alpha/4\pi} \\ (n - i\lambda\alpha/4\pi)\sin d\,\dfrac{2\pi(n - i\lambda\alpha/4\pi)}{\lambda} & \cos d\,\dfrac{2\pi(n - i\lambda\alpha/4\pi)}{\lambda} \end{pmatrix}, \tag{14}$$

where n and d are the refraction index and the thickness of the layer respectively. The transmission coefficient T_{M}[9] of the layer is then given by

$$T_{\mathrm{M}} = \frac{4n_0^2}{(n_0 M_{0,0} + n_0 n_{\mathrm{s}} M_{0,1} + M_{1,0} + n_{\mathrm{s}} M_{1,1})^2}. \tag{15}$$

where n_0 is the superstrate refractive index, and n_{s} is the substrate refractive index of the subcell. The $M_{i,\,j}$ coefficients refer to the matrix transfer elements. Thus, it is possible to determine the incident spectrum on each subcell. The incident photon flux in the GaInP, GaInAs and Ge subcells is given by

$$F_{\mathrm{GaInP}} = T_{\mathrm{ARC}} F_{\mathrm{solar}}, \tag{16}$$

$$F_{\mathrm{GaInAs}} = T_{\mathrm{GaInP}} T_{\mathrm{ARC}} F_{\mathrm{solar}}, \tag{17}$$

$$F_{\mathrm{Ge}} = T_{\mathrm{GaInAs}} T_{\mathrm{GaInP}} T_{\mathrm{ARC}} F_{\mathrm{solar}}, \tag{18}$$

where F_{solar} is the incident photon flux, T_{ARC}, T_{GaInP} and T_{GaInAs} are the transmission coefficients of the anti-reflective coating, the GaInP subcell and the GaInAs subcell, respectively.

This model includes optical and electrical modules, with the optical modules allowing the calculation of the quantity of photons arriving on each junction from the solar spectrum. Then, the electrical model calculates, versus interface recombination velocity, the photocurrents in the space charge region, the emitter and the base for each junction.

3. Solar cell structure and parameters

To calculate the power production of the GaInP/GaInAs/Ge triple-junction cells for space applications, the incident photon flux F_{solar} is taken from a newly proposed reference air mass zero (AM0) spectra (ASTM E-490)[10, 11]. The integrated ASTM E490 AM0 solar spectral irradiance has been made to conform to the value of the solar constant accepted by the space community, which is 1366.1 W/m^2. The transmission coefficient of the anti-reflective coating T_{ARC} (including a 30 nm AlInP top window layer, 52 nm ZnS and 90 nm MgF_2 anti-reflective coating layers), the wavelength-dependent transmission coefficient of the GaInP subcell and the GaInAs subcell are calculated according to Eqs. (14) and (15).

As shown in Fig. 1, a typical two-terminal triple-junction cell for space applications has a Ge bottom cell, a GaInAs middle cell and a GaInP top cell with band gaps of 0.661, 1.405 and 1.85 eV, respectively. The Ge cell is built on the p-type substrate and therefore the base is about 150 μm thick, with a doping concentration of about 6×10^{17} cm^{-3}. The Ge emitter is about 0.3 μm thick with an n-type doping concentration of about 1×10^{19} cm^{-3}. The emitter thickness is 0.1 μm for the other two cells with a doping concentration of about 1×10^{18} cm^{-3}. Since the AM0 spectrum contains relatively more high-energy photons with energy greater than the band gap of the GaInP top cell, the photocurrent of a triple-junction cell with a very thick top cell will generally be limited by that of the middle (GaInAs) cell. Therefore, the middle cell thickness was set to be thick enough (3.6 μm in this paper) with a doping concentration of about 2×10^{17} cm^{-3}, and the top cell thickness was suggested to be about 0.52 μm with a doping concentration of about 1×10^{17} cm^{-3}[12, 13].

The absorption coefficient of GaInP[4] can be fitted by

$$\alpha_{\mathrm{GaInP}} = 5.5\sqrt{E - E_{\mathrm{g}}} + 1.5\sqrt{E - E_{\mathrm{g}} - 1}. \tag{19}$$

The absorption coefficient of GaInAs (with In content of about 0.01)[12] can be fitted by

$$\alpha_{\mathrm{GaInAs}} = 3.3\sqrt{E - E_{\mathrm{g}}}. \tag{20}$$

The direct gap absorption spectra of bulk[14] Ge was used for the calculation

$$\alpha_{\mathrm{Ge}} = 1.9\sqrt{E - E_{\mathrm{g}}^{\Gamma}}\,/E. \tag{21}$$

where E is the photon energy and E_{g} is the fundamental band gap, both in eV, and α in 1/μm.

The diffusion length, the diffusion coefficient and the non-radiative carrier lifetime are calculated according to the doping concentration by using empirical formulas summarized in Ghannam's work[4].

4. Results and discussion

The analysis starts by assuming a recombination velocity of 1×10^6 cm/s at one interface at a time, while that at the other five interfaces is set to zero. Figures 2–4 show the total external quantum efficiencies η and the integrated photocurrent density J_{ph} of the three subcells calculated from Eqs. (1)–(4) using varying values of S_{p} and S_{n}. The external quantum efficiency η is a function of wavelength, and the photocurrent density J_{ph} is obtained from the integral of the product of quantum efficiencies. As shown in the figures, for large absorption coefficients, a high S_{p} causes the blue response to decrease dramatically (see Figs. 2(a), 3(a) and 4(a)). However, a high S_{p} also causes a reduction in the red response as well. In contrast, high S_{n} causes a reduction only in the red response (see Figs. 2(a) and 3(a)), with almost no measurable effect in the blue response for a thick cell (see Fig. 4(a)). The top GaInP cell generates a photocurrent density of 16.44 mA/cm^2 for zero recombination velocity, 15.08 mA/cm^2 for $S_{\mathrm{n}} = 1 \times 10^6$ cm/s, and 13.71 mA/cm^2 for $S_{\mathrm{p}} = 1 \times 10^6$ cm/s (see Fig. 2(b)). The middle GaInAs cell generates a photocurrent density of 17.16 mA/cm^2 for zero recombination velocity, 15.44 mA/cm^2 for S_{n}

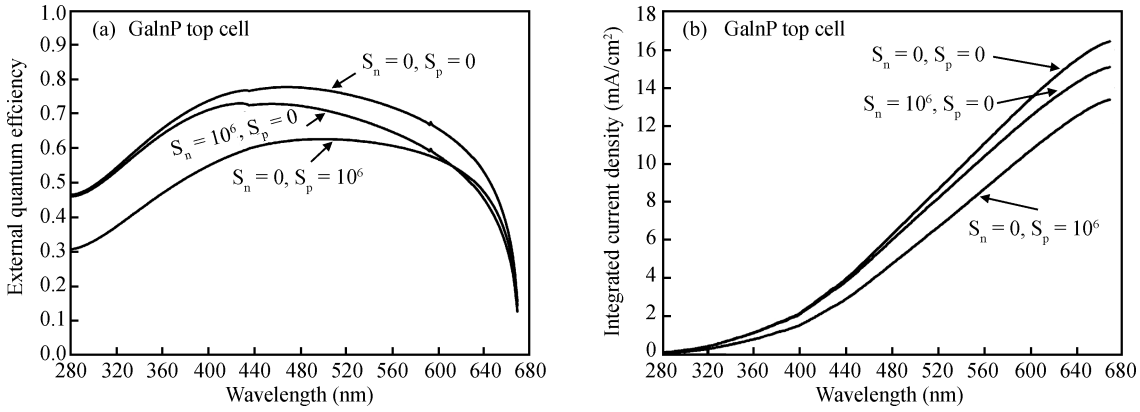

Fig. 2. (a) External quantum efficiency and (b) integrated photocurrent density of the top GaInP cell for various interface recombination velocities as shown in the figures.

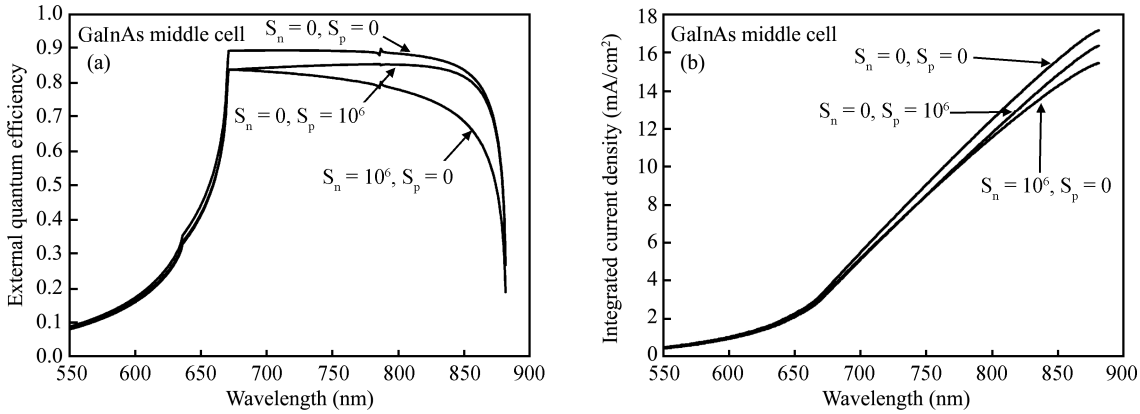

Fig. 3. (a) External quantum efficiency and (b) integrated photocurrent density of the middle GaInAs cell for various interface recombination velocities as shown in the figures.

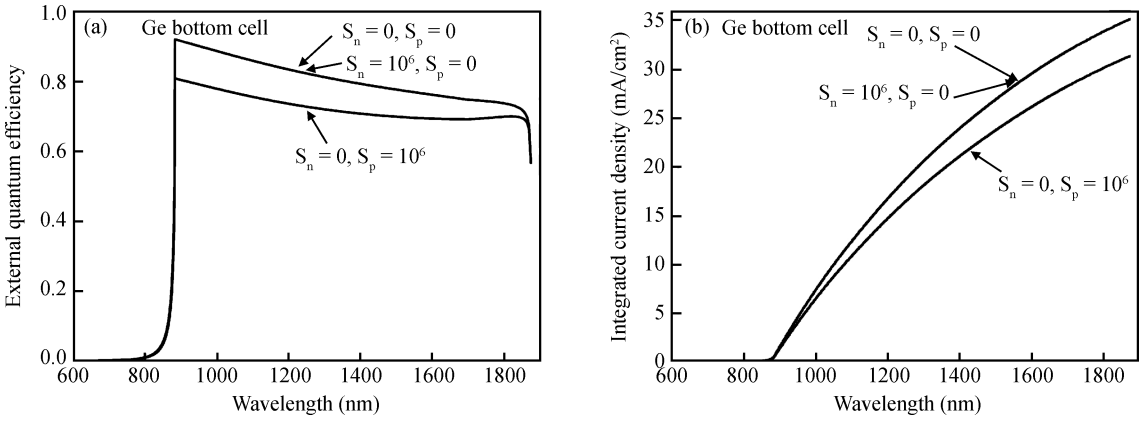

Fig. 4. (a) External quantum efficiency and (b) integrated photocurrent density of the bottom Ge cell for various interface recombination velocities as shown in the figures.

$= 1 \times 10^6$ cm/s, and 16.34 mA/cm^2 for $S_p = 1 \times 10^6$ cm/s (see Fig. 3(b)). The bottom Ge cell generates a photocurrent density of 35.19 mA/cm^2 for zero recombination velocity, 35.19 mA/cm^2 for $S_n = 1 \times 10^6$ cm/s, and 31.41 mA/cm^2 for $S_p = 1 \times 10^6$ cm/s (see Fig. 4(b)).

The short circuit current of the tandem cell is the smallest photocurrent of the subcell. According to Eq. (1), the open-circuit voltage can be obtained as the voltage at which the magnitude of the dark current equals the photocurrents. The corresponding I–V characteristics of the tandem cell are plotted in Fig. 5. The recombination at the back interface of the top cell is very detrimental due to the considerable drop of the cell voltage. The recombination at the back interface of the middle cell and at the emitter surface of the bottom cell also leads to a significant decrease in the cell voltage as shown in Fig. 5. The drop in the cell voltage is less significant for the recombination

Table 1. Figure-of-merits of the tandem cell represented from Fig. 5.

Surface recombination velocity S (cm/s)	Open-circuit voltage V_{oc} (V)	Short-circuit current J_{sc} (A/cm^2)	Fill factor (%)	Tandem cell efficiency (%)
$S = 0$	2.75	0.01644	88.1	29.2
S_n-Ge = 10^6	2.75	0.01644	88.1	29.2
S_p-Ge = 10^6	2.74	0.01644	87.9	29.0
S_n-GaInAs = 10^6	2.70	0.01544	89.4	27.3
S_p-GaInAs = 10^6	2.73	0.01634	87.4	28.5
S_n-GaInP = 10^6	2.65	0.01508	90.9	26.6
S_p-GaInP = 10^6	2.72	0.01371	90.4	24.7

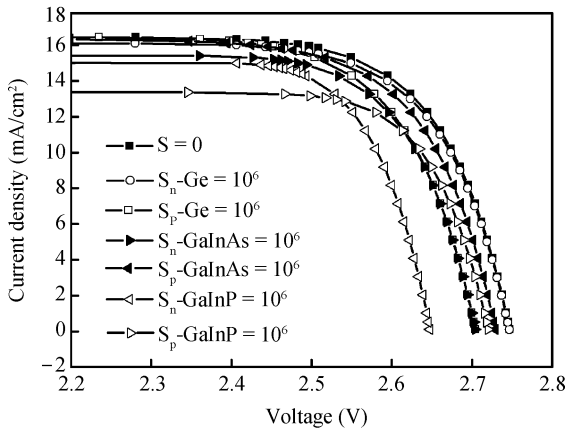

Fig. 5. I–V characteristics of the GaInP/GaInAs/Ge tandem cell under AM0 with recombination velocities at the indicated interfaces and zero elsewhere.

at the emitter surface of the top cell. Since the surface recombination velocity affects both the photocurrents and voltages for each subcell, the fill factors obtained from the I–V curves vary with the surface recombination velocity.

Table 1 represents the figures-of-merit of the tandem cell for various interface recombination velocities. Among all the interfaces, recombination at the emitter surface of the top cell is the most detrimental due to the considerable drop of the cell short circuit current, recombination at the back surface of the top cell is also detrimental due to the considerable drop of the cell voltage. Thus, the surface recombination at the top GaInP cell should be the main limitation for obtaining high efficiency tandem solar cells, while the recombination effect at the back interface of the bottom cell is negligible because the base layer is thick enough. The voltage for each subcell drops with increasing recombination velocity. It varies more significantly with back surface recombination velocity because a large dark current is generated in the base region of the cell with back surface recombination, while the dark current generated in the emitter region of the cell is much smaller (Eqs. (7) and (8)).

In practice, high surface recombination velocities are frequently observed in solar cells. By setting proper surface recombination velocities, the model should predict the external quantum efficiency and illuminated I–V characteristics. Using our model by assuming recombination velocity for a top cell back surface of 1.3×10^5 cm/s, a middle cell back surface of 10^5cm/s and a top cell emitter surface of 5.15×10^4 cm/s[4], we obtained a voltage of 1.38 V for the GaInP subcell, and the theoretical open circuit voltage of the tandem solar cell is about 2.65 V, which is close to that obtained from practical devices[5].

5. Conclusion

The interface recombination effect on the performance of a typical GaInP/GaInAs/Ge tandem solar cell operating under AM0 illumination has been investigated for different recombination velocities at both front and back-surfaces of the three subcells. Recombination at the back interface of the top cell leads to a considerable drop of the cell voltage, while recombination at the back interface of the middle cell and at the emitter surface of the bottom cell leads to a less significant decrease in the cell voltage. Recombination at the emitter surface of the top cell is the most detrimental due to the considerable drop of the cell short circuit current and to a lesser extent to the associated reduction in the cell voltage. Effectively interface passivation of the tandem cell, especially of the top GaInP subcell, should be helpful in achieving high efficiencies.

References

[1] Stan M, Aiken D, Clevenger B, et al. Design and performance of high efficiency III–V space solar cells with monolithic bypass diode architecture. Proceedings of the Fourth World Conference on Photovoltaic Energy Conversion, 2006, 2: 1865

[2] King R R, Fetzer C M, Law D C, et al. Advanced III–V multijunction cells for space. Proceedings of the Fourth World Conference on Photovoltaic Energy Conversion, 2006: 1757

[3] Fetzer C M, King R R, Colter P C, et al. High-efficiency metamorphic GaInP/GaInAs/Ge solar cells grown by MOVPE. J Cryst Growth, 2004, 261: 341

[4] Ghannam M Y, Poortmans J, Nijs J F, et al. Theoretical study of the impact of bulk and interface recombination on the performance of GaInP/GaAs/Ge triple junction tandem solar cells. Proceedings of 3rd World Conference, 2003: 666

[5] Kurtz S R, Olson J M, Friedman D J, et al. Passivation of interfaces in high-efficiency photovoltaic devices. Materials Research Society's Spring Meeting, San Francisco, 1999, NREL/CP-520-26494

[6] Hovel H J. Solar cell. New York: Academic Press, 1975

[7] Fahrenbruch A L, Bube R H. Fundamentals of solar cells photovoltaic solar energy conversion. New York: Academic Press, 1983

[8] Würfel P. Physics of solar cells: from principles to new concepts. Wiley-VCH, 2005

[9] Palik E D. Handbook of optical constants of solids II. San Diego: Academic Press, 1991

[10] Woods T N, Prinz D K, Rottman G J, et al. Validation of the UARS solar ultraviolet irradiances: comparison with the ATLAS 1 and 2 measurements. Journal of the Geophysical Research, 1996, 101: 9541

[11] Neckel H, Labs D. The solar radiation between 3300 and 12500 A. Solar Phys, 1984, 90: 205
[12] Faine P J, Kurtz S R, Olson J M. Modeling of two-junction, series-connected tandem solar cells using top-cell and coating thicknesses as adjustable parameters. Conference Record of the Twenty First IEEE Photovoltaic Specialists Conference, 1990: 339
[13] McMahon W E, Kurtz S R, Emery K, et al. Criteria for the design of GaInP/GaAs/Ge triple-junction cells to optimize their performance outdoors. Proc Conference Record of the Twenty-Ninth IEEE Photovoltaic Specialists Conference, 2002: 931
[14] Hobalen M V. Direct optical transitions from the split-off valence band to the conduction band in germanium. J Phys Chem Solids, 1962, 23: 821